# Mathematical treatment of isotopologue and isotopomer speciation and fractionation in biochemical kinetics

Federico Maggi[1] and William J. Riley[2]*

[1]School of Civil Engineering, The University of Sydney, Sydney 2006, NSW, Australia; [2]Earth Sciences Division, Lawrence Berkeley National Laboratory, Berkeley, CA 94720, USA.

* W.R.'s work was supported by Laboratory Directed Research and Development (LDRD) funding from Berkeley Lab, provided by the Director, Office of Science, of the U.S. Department of Energy under Contract No. DE-AC02-05CH11231.

**Abstract.**

We present a mathematical treatment of the kinetic equations that describe isotopologue and isotopomer speciation and fractionation during enzyme-catalyzed biochemical reactions. These equations, presented here with the name GEBIK (General Equations for Biochemical Isotope Kinetics) and GEBIF (General Equations for Biochemical Isotope Fractionation), take into account microbial biomass and enzyme dynamics, reaction stoichiometry, isotope substitution number, and isotope location within each isotopologue and isotopomer. In addition to solving the complete GEBIK and GEBIF, we also present and discuss two approximations to the full solutions under the assumption of biomass-free and enzyme steady-state, and under the quasi-steady-state assumption as applied to the complexation rate. The complete and approximate approaches are applied to observations of biological denitrification in soils. Our analysis highlights that the full GEBIK and GEBIF provide a more accurate description of concentrations and isotopic compositions of substrates and products throughout the reaction than do the approximate forms. We demonstrate that the isotopic effects of a biochemical reaction depend, in the most general case, on substrate and complex concentrations and, therefore, the fractionation factor is a function of time. We also demonstrate that inverse isotopic effects can occur for values of the fractionation factor smaller than 1, and that reactions that do not discriminate isotopes do not necessarily imply a fractionation factor equal to 1.

## 1. Introduction

Isotopes are widely used in environmental sciences since the magnitude of isotopic enrichment can often be linked with specific processes, and therefore can be used to better understand movement and turnover of chemical compounds within the ecosystem. For example, Perez *et al.* [2006] have observed an average $N_2O$ enrichment of $-74‰$ from nitrification processes and $-23‰$ from denitrification in forested soils. The current mathematical treatment of isotopic effects in biochemical kinetics used to interpret isotopic signatures is based on the pioneering work by Mariotti *et al.* [1981], which has been used in several interpretations of isotopic signature observations [e.g., Van Breukelen *et al.*, 2005; Elsner et al., 2005]. However, this framework has three major limitations: (*i*) the reactions are considered to be first order and exclude the concurrent enzyme and biomass dynamics; (*ii*) the reaction stoichiometry is not explicitly taken into account; (*iii*) isotopologue and isotopomer speciation are not considered. Removing these limitations could improve the interpretation of isotopic signatures and, in a broader context, our understanding of biochemical reactions. In this work we present general equations for biochemical kinetics and isotope speciation and fractionation that address these three limitations.

The first aspect that we include in our treatment is related to the reaction order. Biochemical reactions are widely accepted to occur with order between zero and one, such as in the Michaelis-Menten reaction type [Laidler, 1965]. In this reaction type, the reactants bind to an enzyme to form an activated complex which then releases the final products. The Michaelis-Menten framework, however, assumes a constant enzyme con-

centration and no biomass dynamics. This assumption, also used in recent analytical studies [e.g., Thullner *et al.*, 2008], may lead to incorrect interpretation of isotopic signatures in instances where microbial biomass contributes substantially to the reaction rate via enzyme production. Evidence of the importance of biomass dynamics in relation to reaction velocity has been discussed by Mauclaire *et al.* [2003]. In that work, however, the chemical reaction performed by the biomass was not explicitly linked to the enzyme dynamics. To circumvent these limitations, we explicitly take into account simultaneous enzyme and biomass dynamics under the assumption of transient kinetics as introduced in [Maggi and Riley, 2009] and discussed earlier in Northorp [1980].

The second important aspect we implement in our mathematical treatment is the stoichiometric relationships between reactants and products. Taking into account the reaction stoichiometry is necessary to derive rate constants which mirror the specific velocity of a reaction, and to maintain isotope mass balance along the reaction pathway.

The third aspect introduced in this work is the description of isotopologue and isotopomer kinetics and speciation. More specifically, the location at which an isotope substitution occurs in a product can be used to track which substrate has been consumed and how the product was synthesized during a biochemical reaction. Isotopomer detection has been applied in only a few experimental observations due to the rather complicated techniques involved [e.g., Toyoda *et al.*, 2005; Well *et al.*, 2006]. However, to our knowledge, there is no general approach aimed at modeling kinetic isotopic effects in enzyme-catalyzed reactions in which isotopomer substrates and products intervene simultaneously. To this end, we characterize isotopomer reactions by introducing the number and locations of each isotopic substitution within reacting molecules, and we model iso-

topomer product speciation and fractionation using partitioning coefficients in addition to the stoichiometric coefficients.

The equations presented here have general applicability to describing the components' concentration and isotopic effects and, ideally, could be used in any enzymatically-controlled reaction regardless of the number of substrates, products, microbial strains, and enzymes. Under suitable assumptions, these general equations can be treated in two simplified forms: the first introduces the biomass-free and enzyme-invariant approximation; the second introduces the quasi-steady-state approximation in solving for enzyme-substrate complexation. We demonstrate applications of these equations using isotopic observations of $N_2O$ production and consumption from the experiments by Mariotti *et al.* [1981] and Menyailo and Hungate [2006].

## 2. General Equations for Biochemical Isotope Kinetics (GEBIK)

To present the kinetic equations describing isotope kinetics in biochemical reactions, we first introduce the notation used to define the isotopic expression of a molecule, and we next present examples to help the reader throughout the remainder of the paper.

### 2.1. Notation

We define S and P to be the generic substrate and product molecules that are consumed and produced during a reaction, respectively, and the italic character $S$ and $P$ to be the concentrations of S and P. Both S and P molecules contain at least one isotopic expression of the tracer atom used to assess the isotopic effect of a reaction. For simplicity, we limit to two the number of isotopic expressions for a tracer element, though the notation can be applied to any number of isotopic expressions. For instance, if the carbon element is

used as a tracer, both S and P contain at least one C atom, which can appear in not more than two isotopic forms, e.g., $^{12}$C and $^{13}$C. We use the left subscript notation to indicate the total number of tracer atoms, and the left superscript to indicate the number of isotopic substitutions in the same molecule. In this way, ${}^{b}_{a}$S means that the substrate molecule S contains $_a$ atoms of tracer (rare plus abundant), and that $^b$ atoms have been substituted with the rare isotopic expression of the tracer. The condition $0 \leq b \leq a$ has to be satisfied. For example, if the rare stable nitrogen isotope $^{15}$N is used in the reaction $^{15}$N$^{14}$NO $\rightarrow$ $^{15}$N$^{14}$N, both substrate ${}^{1}_{2}$S and product ${}^{1}_{2}$P have $a = 2$ nitrogen atoms, $b = 1$ atom being substituted with the rare isotope $^{15}$N. Note that our notation of the chemical reactions takes into account the mass and molar balance of the isotope tracers but not of other elements. This approach, however, does not affect our mathematical treatment of isotope kinetics and fractionation.

Substrates and products appear in a chemical reaction with specific stoichiometric coefficients. When chemical reactions comprise combinations of reactants and products with various isotopic expressions, the stoichiometric coefficients are functions of the isotope substitution number. If $x_b$ and $y_d$ are the stoichiometric coefficient for ${}^{b}_{a}$S substrate and ${}^{d}_{c}$P product, we can write

$$\sum_{b=0}^{a} x_b \, {}^{b}_{a}\mathrm{S} \rightarrow \sum_{d=0}^{c} y_d \, {}^{d}_{c}\mathrm{P}.$$

For example, in the reaction $^{14}NO_3^- + {}^{15}NO_3^- \rightarrow {}^{14}N^{15}NO$, our notation becomes ${}^{0}_{1}\mathrm{S} + {}^{1}_{1}\mathrm{S} \rightarrow {}^{1}_{2}\mathrm{P}$, with $x_0 = x_1 = 1$ for both isotopologue reactants of the same substrate with substitution number $b = 0$ and $b = 1$, and with $y_1 = 1$ for ${}^{1}_{2}$P and $y_0 = y_2 = 0$ because the reaction does not comprise production of ${}^{0}_{2}\mathrm{P} = {}^{14}\mathrm{N}_2\mathrm{O}$ and ${}^{2}_{2}\mathrm{P} = {}^{15}\mathrm{N}_2\mathrm{O}$.

The tracer element in a multiatomic molecule with multiple atoms of the same tracer may occupy diverse locations, i.e., it can have different isotopomer expressions. We indicate the location of the tracer element with a Greek symbol as right superscript, so that the isotopomer reactants ${}^{b}_{a}\mathrm{S}^{\beta}$ and ${}^{b}_{a}\mathrm{S}^{\gamma}$ will be different expressions of the same isotopologue ${}^{b}_{a}\mathrm{S}$. Isotopomers only exist when $1 \leq b < a$ and $a \geq 2$. The substitution location has to be specifically defined depending on the number of tracer atoms $a$, number of substitutions $b$, and molecule structure. For multiatomic molecules that are symmetric with respect to tracer position, there is no need to specify the substitution position when $b = 1$. For example, one substitution of deuterium $\mathrm{D} = {}^{2}\mathrm{H}$ in the symmetric methane molecule $\mathrm{CDH_3}$ does not require the use of the right superscript. In the case that $b = 2$, the substitution location has to be specified, while for $\mathrm{CHD_3}$ and $\mathrm{CD_4}$ it is not required. For example, two D substitutions in $\mathrm{CD_2H_2}$ can occur in adjacent or non-adjacent locations. Using this notation, the reaction

$$\mathrm{CD_2H_2} + 2\mathrm{O_2} \rightarrow \mathrm{H_2O} + \mathrm{D_2O} + \mathrm{CO_2},$$

can be written as ${}^{2}_{4}\mathrm{S}^{\beta} \rightarrow {}^{0}_{2}\mathrm{P} + {}^{2}_{2}\mathrm{P}$, where the $\beta$ expression in ${}^{2}_{4}\mathrm{S}^{\beta}$ defines only one of the two methane forms (either with adjacent or non-adjacent D atoms). The location of D in the two isotopologue water molecules produced on the right-hand side of the reaction has not been indicated because D is present in only one water molecule at saturation, and because the water molecule is symmetric. For asymmetric and multiatomic molecules with $1 \leq b < a$ and $a \geq 2$, definition of the substitution location is always required. For instance, the isotopomers of the (asymmetric) nitrous oxide molecule $\mathrm{N_2O}$ are ${}^{1}_{2}\mathrm{S}^{\beta} = {}^{15}\mathrm{N}{}^{14}\mathrm{NO}$ and ${}^{1}_{2}\mathrm{S}^{\gamma} = {}^{14}\mathrm{N}{}^{15}\mathrm{NO}$.

When the isotopomer products are asymmetric molecules, a number of isotopomer reactions should be written, each describing production of a different isotopomer from the same reactants. A convenient way to take into account isotopomer formation is to introduce a partitioning coefficient, $u$, linked to each isotopomer expression, and generalized as

$$\sum_{b=0}^{a}\sum_{\beta} x_b \, {}^{b}_{a}\mathrm{S}^{\beta} \rightarrow \sum_{d=0}^{c}\sum_{\gamma} u_\gamma y_d \, {}^{d}_{c}\mathrm{P}^{\gamma},$$

where $\sum_\beta$ and $\sum_\gamma$ are expressed over the possible combinations of locations for $b$ and $d$ substitution numbers, with $\sum_\gamma u_\gamma = 1$. For example, using N isotopes as tracers, the isotopomer reactions

$$^{14}\mathrm{NO}_3^- + {}^{15}\mathrm{NO}_3^- \rightarrow {}^{14}\mathrm{N}^{15}\mathrm{NO},$$

$$^{14}\mathrm{NO}_3^- + {}^{15}\mathrm{NO}_3^- \rightarrow {}^{15}\mathrm{N}^{14}\mathrm{NO},$$

can be written as one reaction in which each isotopomer product is multiplied by its partition coefficient as

$${}^{0}_{1}\mathrm{S} + {}^{1}_{1}\mathrm{S} \rightarrow u_\beta \, {}^{1}_{2}\mathrm{P}^{\beta} + u_\gamma \, {}^{1}_{2}\mathrm{P}^{\gamma},$$

with $u_\gamma = 1 - u_\beta$.

More generally, the tracer element does not necessarily occur in only one substrate and one product. If $n_S$ substrates react releasing $n_P$ products, each having an isotopic expression of the tracer element, then we can write

$$\sum_{j=1}^{n_S}\sum_{b_j=0}^{a_j}\sum_{\beta_j} x_{b_j} \, {}^{b_j}_{a_j}\mathrm{S}_j^{\beta_j} \rightarrow \sum_{h=1}^{n_P}\sum_{d_h=0}^{c_h}\sum_{\gamma_h} u_{\gamma_h} \; y_{d_h} \, {}^{d_h}_{c_h}\mathrm{P}_h^{\gamma_h}. \qquad (2)$$

For instance, consider the $^{16}O$ and $^{18}O$ tracers in the reaction $CH_2{}^{18}O + {}^{16}O_2 \rightarrow H_2{}^{16}O + C^{18}O^{16}O$; in this case the reaction can be written as ${}^1_1S_1 + {}^0_2\,S_2 \rightarrow {}^0_1P_1 + {}^1_2P_2$ with two substrates and two products without indication of the substitution location because all molecules are symmetric.

## 2.2. Isotope balances

Regardless of the number of reacting substrates and released products, the principle of mass conservation relative to the tracer isotopes has to be satisfied within a multimolecular and multiatomic reaction. Using the notation introduced in Eq. (2), the following isotope balances have to hold

$$\sum_{j=1}^{n_S}\sum_{b_j=0}^{a_j}\sum_{\beta_j} x_{b_j}\, a_j = \sum_{h=1}^{n_P}\sum_{d_h=0}^{c_h}\sum_{\gamma_h} u_{\gamma_h}\, y_{d_h}\, c_h, \tag{3a}$$

$$\sum_{j=1}^{n_S}\sum_{b_j=0}^{a_j}\sum_{\beta_j} x_{b_j}\, b_j = \sum_{h=1}^{n_P}\sum_{d_h=0}^{c_h}\sum_{\gamma_h} u_{\gamma_h}\, y_{d_h}\, d_h. \tag{3b}$$

## 2.3. Biochemical reactions

Biochemical kinetic reactions are often catalytic reactions in which one or more substrates, $S_j$, bind to an enzyme, E, to form a reversible activated complex, C, which releases one or more products, $P_h$, and free, unchanged enzyme. This representation of biochemical enzymatic reactions was proposed in 1913 and is known as Michaelis-Menten kinetics [Laidler, 1965]. This approach is generalized in this section to account for substrate and product isotopologue and isotopomer expressions, and for the stoichiometric relationships among them. To this end, we consider $m$ reactions, each describing the reaction among reactants with different isotopic expressions and the release of products

with different isotopic expressions. Generalizing Eq. (2) for a set of $m$ reactions, and using the Michaelis-Menten complexation framework, we obtain for each reaction

$$\sum_{j=1}^{n_S}\sum_{b_{ji}=0}^{a_{ji}}\sum_{\beta_{ji}} x_{b_{ji}} \, {}^{b_{ji}}_{a_j}\mathrm{S}_j^{\beta_{ji}} + \mathrm{E} \underset{\mathrm{k}_{2(i)}}{\overset{\mathrm{k}_{1(i)}}{\rightleftarrows}} \mathrm{C}_i \tag{4a}$$

$$\mathrm{C}_i \xrightarrow{\mathrm{k}_{3(i)}} \sum_{h=1}^{n_P}\sum_{d_{hi}=0}^{c_{hi}}\sum_{\gamma_{hi}} u_{\gamma_{hi}} y_{d_{hi}} \, {}^{d_{hi}}_{c_h}\mathrm{P}_h^{\gamma_{hi}} + \mathrm{E}, \tag{4b}$$

where $i = 1, ..., m$ identifies the reaction, $j$ identifies the substrate, $h$ identifies the product, and $\mathrm{k}_{1(i)}$, $\mathrm{k}_{2(i)}$, and $\mathrm{k}_{3(i)}$ are the rate constants indexed for each of the $m$ reactions. The value of $m$ has to be consistent with the number of combinations between stoichiometric coefficients ($x$ and $y$), number of tracer atoms in substrates and products ($a$ and $c$), number of substitutions ($b$ and $d$), and number of different locations of the substituted atoms ($\beta$ and $\gamma$), see *Example 1.*

- *Example 1.* Consider the $^{15}$N and $^{14}$N isotopes in the reaction 2 $\mathrm{NO_3^-} \rightarrow \mathrm{N_2O}$ which comprises one or multiple isotopologue reactants of one substrate (i.e., $j = 1$) and one product (i.e., $h = 1$). The $m = 4$ isotopologue and isotopomer reactions are

$$2\,{}^{14}\mathrm{NO_3^-} \rightarrow {}^{14}\mathrm{N_2O}, \tag{5a}$$

$${}^{14}\mathrm{NO_3^-} + {}^{15}\mathrm{NO_3^-} \rightarrow {}^{14}\mathrm{N}{}^{15}\mathrm{NO}, \tag{5b}$$

$${}^{14}\mathrm{NO_3^-} + {}^{15}\mathrm{NO_3^-} \rightarrow {}^{15}\mathrm{N}{}^{14}\mathrm{NO}, \tag{5c}$$

$$2\,{}^{15}\mathrm{NO_3^-} \rightarrow {}^{15}\mathrm{N_2O}, \tag{5d}$$

while their symbolic representation using Eqs. (4) is

$$2\,{}^{0}_{1}\mathrm{S} \quad + \mathrm{E} \underset{\mathrm{k}_{2(1)}}{\overset{\mathrm{k}_{1(1)}}{\rightleftarrows}} \mathrm{C}_1 \xrightarrow{\mathrm{k}_{3(1)}} {}^{0}_{2}\mathrm{P} + \mathrm{E}, \tag{6a}$$

$${}^{0}_{1}\mathrm{S} + {}^{1}_{1}\mathrm{S} + \mathrm{E} \underset{\mathrm{k}_{2(2)}}{\overset{\mathrm{k}_{1(2)}}{\rightleftarrows}} \mathrm{C}_2 \xrightarrow{\mathrm{k}_{3(2)}} u_\beta\,{}^{1}_{2}\mathrm{P}^{\beta} + u_\gamma\,{}^{1}_{2}\mathrm{P}^{\gamma} + \mathrm{E}, \tag{6b}$$

$$2\,{}^{1}_{1}\mathrm{S} + \mathrm{E} \underset{\mathrm{k}_{2(3)}}{\overset{\mathrm{k}_{1(3)}}{\rightleftarrows}} \mathrm{C}_3 \xrightarrow{\mathrm{k}_{3(3)}} {}^{2}_{2}\mathrm{P} + \mathrm{E}, \tag{6c}$$

where the reaction in Eq. (6b) describes both isotopomer products $\mathrm{P}^{\beta}$ and $\mathrm{P}^{\gamma}$. Notice that the isotopomer treatment introduced with the partition coefficients $u_\beta$ and $u_\gamma = (1 - u_\beta)$ allows us to eliminate biochemical reactions, decrease the number of rate constants and, therefore, simplify the kinetic equations as shown in the following examples.

### 2.4. Generalized kinetic equations

In the Michaelis-Menten approach described above, the total enzyme concentration was assumed to be constant over time, and, under the quasi-steady-state hypothesis applied to the concentration of C, the kinetic equations describing S and P could be written in a simplified form. In a recent work, Maggi and Riley [2009] have coupled the Michaelis-Menten equations describing chemical kinetics with the Monod kinetics [Monod, 1949] describing biomass dynamics, under the assumption that the enzyme concentration is proportional to the biomass concentration and that the reaction is not in quasi-steady state. This approach, described in Maggi and Riley [2009] under the name of transient Michaelis-Menten-Monod kinetics, is generalized here to describe the kinetics of biomass and enzyme-mediated isotopologue and isotopomer speciation and fractionation.

We assume that the system is closed to mass transfer; therefore the total mass of each tracer in S, C, and P in Eq. (4) is conserved through time. In addition, we assume that the total enzyme concentration (free plus bound in the complexes $C_i$), is proportional to

the biomass concentration, $B$, through the enzyme yield coefficient, $z$, as $zB$. Assuming that the initial concentrations of all complexes and products in Eqs. (4) are zero at time $t = 0$, the following molar conservation law for the chemical components in each reaction and mass conservation low for biomass and enzyme can be written

$$\frac{{}^{b_{ji}}_{a_j}S_j^{\beta_{ji}}(0)}{x_{b_{ji}}} = \frac{{}^{b_{ji}}_{a_j}S_j^{\beta_{ji}}(t)}{x_{b_{ji}}} + C_i(t) + \frac{\displaystyle\sum_{h=1}^{n_P}\sum_{d_{hi}=0}^{c_{hi}}\sum_{\gamma_{hi}} u_{\gamma_{hi}} y_{d_{hi}}\, {}^{d_{hi}}_{c_h}\mathrm{P}_h^{\gamma_{hi}}}{\displaystyle\sum_{h=1}^{n_P}\sum_{d_{hi}=0}^{c_{hi}}\sum_{\gamma_{hi}} u_{\gamma_{hi}} y_{d_{hi}}}, \tag{7a}$$

$$zB(t) = E(t) + \sum_{i=1}^{m} C_i(t), \tag{7b}$$

with the coefficients $x_{b_{ji}} > 0$, $y_{d_{hi}} > 0$ and $u_{\gamma_{hi}} > 0$ in Eq. (7a), and with $E(t)$ in Eq. (7b) being the free enzyme concentration at time $t$. Equation (7b) states that the $m$ reactions are coupled to each other via the complexes $C_i$ (the number of complexes equals the number of reactions), thereby introducing competitive substrate consumption.

The rate of change of each substrate $S_j$ for each isotopic expression $b_j$ and $\beta_j$, each complex $C_i$, and each product $P_h$ for each isotopic expression $c_h$ and $d_h$ in Eqs. (4) can be expressed as a function of the rate constants $\mathrm{k}_{1(i)}$, $\mathrm{k}_{2(i)}$ and $\mathrm{k}_{3(i)}$, and as a function of the product of the reactants' concentrations. This product also defines the reaction order. For reactions with multiple reactants, however, there exists no first-principle method to determine the reaction order, that is, how many reactants and to which power (in some cases the stoichiometric coefficients) have to be used in writing the kinetic equations [McNaught and Wilkinson, 1997; Atkins, 1998]. In isotopic applications, the number of reactants may become exceedingly large due to their isotopologue expressions, therefore

taking the product of each reactant concentration to the power of their stoichiometric coefficient may lead to incorrect description of the reaction order. An empirical rule that we propose here is to describe chemical kinetics in terms of the concentration of the two most limiting reactants. This rule returns kinetic equations that are analogous to the classic Michaelis-Menten kinetics. We assume therefore that the substrate kinetics are always determined by the enzyme concentration $E$ (required for the reaction) and the reactant with the lowest concentration within each of the $m$ reactions. We define by $\overline{S}_i$ the most limiting reactant substrate among ${}^{b_{ji}}_{a_j}S_j^{\beta_{ji}}$ in the $i$th reaction of Eqs. (4). For example, the limiting reactants in the isotopologue reactions of Eqs. (5b) and (5c) are $E$ and ${}^{15}\mathrm{NO}_3^-$.

For each substrate $j$, activated complex $i$, product $h$, enzyme $E$, and biomass $B$, we can write the following kinetic equations

$$\frac{\mathrm{d}[{}^{b_j}_{a_j}S_j^{\beta_j}]}{\mathrm{d}t} = \sum_i x_{b_{ji}}[\mathrm{k}_{2(i)}C_i - \mathrm{k}_{1(i)}E\overline{S}_i], \tag{8a}$$

$$\frac{\mathrm{d}C_i}{\mathrm{d}t} = \mathrm{k}_{1(i)}E\overline{S}_i - [\mathrm{k}_{2(i)} + \mathrm{k}_{3(i)}]C_i, \tag{8b}$$

$$\frac{\mathrm{d}[{}^{d_h}_{c_h}P_h^{\gamma_h}]}{\mathrm{d}t} = \sum_i u_{\gamma_{hi}}y_{d_{hi}}\mathrm{k}_{3(i)}C_i, \tag{8c}$$

$$\frac{\mathrm{d}E}{\mathrm{d}t} = z\frac{\mathrm{d}B}{\mathrm{d}t} - \sum_i \frac{\mathrm{d}C_i}{\mathrm{d}t}, \tag{8d}$$

$$\frac{\mathrm{d}B}{\mathrm{d}t} = Y\sum_h\sum_{d_h}\sum_{\gamma_h}\frac{\mathrm{d}[{}^{d_h}_{c_h}P_h^{\gamma_h}]}{\mathrm{d}t} - \mu B. \tag{8e}$$

The enzyme dynamics in Eq. (8d) are obtained by taking the first derivative of the mass conservation law in Eq. (7b). Equation (8e) describes microbial biomass dynamics by means of multiple Monod kinetics, with $Y$ the yield coefficient expressing the biomass gain per unit of released product and $\mu$ expressing the biomass mortality rate [Monod,

1949]. Because $B$ is assumed to increase in response to the release of the products $P_h$, and because enzyme and biomass concentrations are linearly dependent, Eq. (8d) implies that the enzyme is synthesized at the same rate as biomass growth and deteriorates at the same rate as microbial death. The kinetic equations presented above do not imply any specific assumption on where complexation occurs exactly, that is, whether enzyme-substrate binding occurs inside, outside, or within the cell membrane. It is assumed, rather, that Eqs. (8) describe the reactions as they occur at scales much larger than the cell scale and that, therefore, the enzyme concetration is the bulk concetration. This approach, though simplifying the enzyme dynamics, improves the original Michaelis-Menten formulation by which the total enzyme concentration, $E+\sum_i C_i$, was assumed constant over time and not linked to any microbial biomass dynamics [Haldane, 1930]. Finally, biomass is assumed to not immobilize substrates or products for cell maintenance or incorporation into new biomass and, therefore, no fractionation was assumed to occur within the biomass.

Eqs. (8) are presented here for only one microbial functional group and one enzyme. However, the same biochemical system can be further generalized to include any number of microbial group and for multiple enzymes for each function group.

Eqs. (8) cannot be solved analytically and must therefore be solved numerically. Approximate solutions to Eqs. (8) are possible under specific assumptions that are discussed later.

We refer to Eqs. (8) as the General Equations for Biochemical Isotope Kinetics (GEBIK).

## 3. General Equations for Biochemical Isotope Fractionation (GEBIF)

In this section we introduce the equations describing the isotopic composition of the components within a biochemical system and the isotopic effects produced by the reaction.

### 3.1. Isotopic ratio and isotopic composition

The isotopic composition of the components in the biochemical system of Eqs. (4) can be defined in different ways depending on the definition of isotopic ratio. Three definitions are described here: $(i)$ isotopic ratio relative to each component in the system, each with its isotopic expression, with respect to the concentration of its most abundant isotopologue; $(ii)$ isotopic ratio relative to the mass of the tracer element in each component; and $(iii)$ isotopic ratio relative to the mass of the tracer element in the accumulated substrates and products.

The isotopic ratio in definition $(i)$ relative to each component in the system can be calculated from the ratio between the concentration of that component (with substitution numbers $0 < b_j \leq a_j$ and $0 < d_k \leq c_k$) and the concentration of its most abundant isotopologue expression (i.e., with $b_j = 0$ and $d_k = 0$) as

$$R^{**}_{S_{b_j,\beta_j}}(t) = \frac{{}^{b_j}_{a_j}S_j^{\beta_j}(t)}{{}^{0}_{a_j}S_j(t)}, \tag{9a}$$

$$R^{**}_{P_{d_h,\gamma_h}}(t) = \frac{{}^{d_h}_{c_h}P_h^{\gamma_h}(t)}{{}^{0}_{c_h}P_h(t)}, \tag{9b}$$

where each concentration is computed from the GEBIK Eqs. (8). The double star ($^{**}$) is the marker used to differentiate the isotopic ratios in this definition from the other definitions. For instance, if one wished to assess the isotopic ratio of $N_2O$ product from nitrate $NO_3^-$ reactant using N as a tracer, the ratio $^{15}N^{14}NO/^{14}N_2O$ can be calculated from Eq. (9b), while the isotopic ratio $^{15}NO_3^-/^{14}NO_3^-$ can be calculated from Eq. (9a). However, it

is not currently possible to experimentally assess with ease the number and substitution locations in a specific molecule with mass spectrometry analyses. More specifically, $N_2O$ can occur with four isotopic expressions as described in Eqs. (5). Mass spectrometry can return the mass of $^{15}N$ and $^{14}N$ in $N_2O$ but does not indicate how $^{14}N$ and $^{15}N$ are distributed among the fours isotopic expressions of $N_2O$. For comparison with experimental data, therefore, it may be convenient to use the isotopic ratios expressed as functions of the mass of the tracer element of definition $(ii)$.

The isotopic ratios in definition $(ii)$ for the relative mass of the tracer element in each component within the system requires the molecular weight of each substrate, ${}^{b_j}M_{S_j}$, and product, ${}^{d_h}M_{P_h}$, accounting for the substitution numbers $b_j$ and $d_h$, respectively. Defining the atomic weight of the abundant isotope with $p$, and of the rare isotope with $q > p$, the isotopic ratios become

$$R^*_{S_j}(t) = \frac{\displaystyle\sum_{b_j \neq 0} \sum_{\beta_j} \frac{b_j q}{{}^{b_j}M_{S_j}} \, {}^{b_j}_{a_j}S_j^{\beta_j}(t)}{\displaystyle\sum_{b_j \neq a_j} \sum_{\beta_j} \frac{(a_j - b_j)p}{{}^{b_j}M_{S_j}} \, {}^{b_j}_{a_j}S_j^{\beta_j}(t)}, \tag{10a}$$

$$R^*_{P_h}(t) = \frac{\displaystyle\sum_{d_h \neq 0} \sum_{\gamma_h} \frac{d_h q}{{}^{d_h}M_{P_h}} \, {}^{d_h}_{c_h}P_h^{\gamma_h}(t)}{\displaystyle\sum_{d_h \neq c_h} \sum_{\gamma_h} \frac{(c_h - d_h)p}{{}^{d_h}M_{P_h}} \, {}^{d_h}_{c_h}P_h^{\gamma_h}(t)}, \tag{10b}$$

where star (*) is introduced to differentiate the isotopic ratios defined here from the other definitions. Equations (10) can generally be used for comparison with mass spectrometry data if the various $j$ substrates and $h$ products can be separated with ease. If this is not possible, a convenient way to interpret isotopic compositions from experimental

observations is to compute the cumulative isotopic ratios relative to the tracer element as in definition (*iii*).

Definition (*iii*) for the cumulative isotopic ratios relative to the mass of the tracer element can be derived from Eqs. (10) by accumulating the mass of the tracer element in all isotopologue substrate and product expressions as

$$R_S(t) = \frac{\sum_j \sum_{b_j \neq 0} \sum_{\beta_j} \frac{b_j q}{{}^{b_j}M_{S_j}} \, {}^{b_j}_{a_j}S_j^{\beta_j}(t)}{\sum_j \sum_{b_j \neq a_j} \sum_{\beta_j} \frac{(a_j - b_j)p}{{}^{b_j}M_{S_j}} \, {}^{b_j}_{a_j}S_j^{\beta_j}(t)}, \tag{11a}$$

$$R_P(t) = \frac{\sum_h \sum_{d_h \neq 0} \sum_{\gamma_h} \frac{d_h q}{{}^{d_h}M_{P_h}} \, {}^{d_h}_{c_h}P_h^{\gamma_h}(t)}{\sum_h \sum_{d_h \neq c_h} \sum_{\gamma_h} \frac{(c_h - d_h)p}{{}^{d_h}M_{P_h}} \, {}^{d_h}_{c_h}P_h^{\gamma_h}(t)}. \tag{11b}$$

Eqs. (11) become equal to Eqs. (10) if there is only one substrate ($j = 1$) and one product ($h = 1$). For practical reasons, and for the higher degree of generalization, we will use definition (*iii*) of the isotopic ratios in the remainder of the paper keeping in mind that, nevertheless, definitions (*i*) and (*ii*) can also be used. An application of Eqs. (11) is shown in *Example 3*.

It is common to describe the isotopic composition in ‰ relative to a standard, $R_{std}$, as $\delta = (R/R_{std} - 1)1000$. Using the isotopic ratios of Eqs. (11), the isotopic compositions become

$$\delta_S(t) = \left(\frac{R_S(t)}{R_{std}} - 1\right) 1000, \tag{12a}$$

$$\delta_P(t) = \left(\frac{R_P(t)}{R_{std}} - 1\right) 1000. \tag{12b}$$

Similar definitions of isotopic compositions can be derived using the isotopic ratios in Eqs. (9) and Eqs. (10).

• *Example 3.* For the biochemical system used in *Example 1* with S = $NO_3^-$ and P = $N_2O$, the isotopic ratios of Eqs. (11) are

$$R_S(t) = \frac{15/63\ {}^1_1S(t)}{14/62\ {}^0_1S(t)}, \tag{13a}$$

$$R_P(t) = \frac{15/45\ {}^1_2P(t) + 30/46\ {}^2_2P(t)}{28/44\ {}^0_2P(t) + 14/45\ {}^1_2P(t)}, \tag{13b}$$

where ${}^1_2P(t) = {}^1_2P^\beta(t) + {}^1_2P^\gamma(t)$. The concentration of each component can be calculated using the GEBIK Eqs (8).

### 3.2. Fractionation factor

The isotopic ratio of the product in Eq. (11b) can be used to define the instantaneous isotopic ratio, $IR_P(t)$ as

$$IR_P(t) = \frac{\displaystyle\sum_h \sum_{d_h \neq 0} \sum_{\gamma_h} \frac{d_h q}{{}_{d_h}M_{P_h}} \frac{\mathrm{d}[{}^{d_h}_{c_h}P_h^{\gamma_h}(t)]}{\mathrm{d}t}}{\displaystyle\sum_h \sum_{d_h \neq c_h} \sum_{\gamma_h} \frac{(c_h - d_h)p}{{}_{d_h}M_{P_h}} \frac{\mathrm{d}[{}^{d_h}_{c_h}P_h^{\gamma_h}(t)]}{\mathrm{d}t}}, \tag{14}$$

where the rate of change $\mathrm{d}[{}^{d_h}_{c_h}P_h^{\gamma_h}(t)]/\mathrm{d}t$ is defined in GEBIK Eq. (8c) for each product, each with an isotopic expression of the tracer element. The ratio $IR_P(t)$ describes the isotopic ratio of the increment of product concentration relative to the mass of tracer element over the infinitesimal time interval $\mathrm{d}t$.

Combining Eq. (14) with the cumulative isotopic ratio of the substrate $R_S(t)$ of Eq. (11a) as proposed in Mariotti *et al.* [1981], we obtain the fractionation factor relative to the tracer element

$$\alpha(t) = \frac{IR_P(t)}{R_S(t)}. \tag{15}$$

Equation (15) describes the most general case of bulk isotopic effects which the tracer element is subject to in biochemical reactions of the type in Eq. (4).

Because of their general applicability, we refer to the isotopic ratios in Eq. (11), the instantaneous isotopic ratio of Eq. (14), and the fractionation factor in Eq. (15) as the General Equations for Biochemical Isotope Fractionation (GEBIF). Two applications of GEBIF are shown in *Example 4* and *5* to calculate the fractionation factor $\alpha$.

• *Example 4.* For the biochemical reactions in *Example 1* we calculate the instantaneous isotopic ratio of the product using Eq. (14) as

$$\begin{aligned} IR_P(t) &= \frac{15/45\ \mathrm{d}[{}^1_2P] + 30/46\ \mathrm{d}[{}^2_2P]}{28/44\ \mathrm{d}[{}^0_2P] + 14/45\ \mathrm{d}[{}^1_2P]} = \\ &= \frac{165}{161}\ \frac{23\ \mathrm{k}_{3(2)}C_2(t) + 45\ \mathrm{k}_{3(3)}C_3(t)}{45\ \mathrm{k}_{3(1)}C_1(t) + 22\ \mathrm{k}_{3(2)}C_2(t)}, \end{aligned} \tag{16}$$

with $\mathrm{d}[{}^1_2P(t)]/\mathrm{d}t = \mathrm{d}[{}^1_2P^\beta(t)]/\mathrm{d}t + \mathrm{d}[{}^1_2P^\gamma(t)]/\mathrm{d}t$. The rate of change of the product concentrations are written using the GEBIK equations.

In a similar way, we compute the isotopic ratio of the substrate, $R_S$, using Eq. (11a), which is already given in Eq. (13a) of *Example 3*. Substituting Eq. (13a) and (16) into the definition of $\alpha(t)$ in Eq. (15) we obtain

$$\alpha(t) = \frac{693}{713}\frac{[23\ \mathrm{k}_{3(2)}C_2(t) + 45\ \mathrm{k}_{3(3)}C_3(t)]\ {}^0_1S(t)}{[45\ \mathrm{k}_{3(1)}C_1(t) + 22\ \mathrm{k}_{3(2)}C_2(t)]\ {}^1_1S(t)}. \tag{17}$$

• *Example 5.* If we simplify *Example 1* by using only the first and third reactions, that is, excluding the isotopomer reaction $i = 2$, then we obtain

$$IR_P(t) = \frac{165}{161}\frac{\mathrm{k}_{3(3)}}{\mathrm{k}_{3(1)}}\frac{C_3(t)}{C_1(t)}, \tag{18}$$

$$\alpha(t) = \frac{693}{713}\frac{\mathrm{k}_{3(3)}C_3(t)}{\mathrm{k}_{3(1)}C_1(t)}\frac{{}^0_1S(t)}{{}^1_1S(t)}. \tag{19}$$

Equations (17) and (19) show that the isotopic effects are not steady, but rather change over time with the ratio of complex and substrate concentrations.

## 4. Approximate GEBIK and GEBIF

GEBIK and GEBIF fully characterize the reaction rate, speciation, and fractionation (i.e., the isotopic effect) of each component in a biochemical reaction taking into account the number of substrates and products, isotopologue and isotopomer expressions, and the enzyme and biomass dynamics. Nonetheless, a number of assumptions allow us to derive simpler, approximate forms of GEBIK and GEBIF. In the following sections we present two mathematical treatments corresponding to: $(i)$ the biomass-free and enzyme-invariant (steady state) assumption (BFEI); and $(ii)$ the quasi-steady state assumption (QSS) in which the complex concentrations $C_i$ are assumed to be constant ($\mathrm{d}C_i/\mathrm{d}t = 0$) [Haldane, 1930; Laidler, 1965].

### 4.1. Biomass-Free and Enzyme-Invariant (BFEI) treatment

In instances where the biomass and enzyme concentrations are not appreciably changing in time, we can assume that biomass dynamics is negligible and that the total enzyme concentration is constant. These assumptions are referred here to as biomass-free and enzyme-invariant (BFEI). The mass conservation laws of Eq. (7b) simplify to

$$E_0 = E(t) + \sum_i C_i(t), \tag{20}$$

and the GEBIK equations become

$$\frac{\mathrm{d}[{}^{b_j}_{a_j}S_j^{\beta_j}]}{\mathrm{d}t} = \sum_i x_{b_{ji}}[\mathrm{k}_{2(i)}C_i - \mathrm{k}_{1(i)}E\overline{S}_i], \tag{21a}$$

$$\frac{\mathrm{d}C_i}{\mathrm{d}t} = \mathrm{k}_{1(i)}E\overline{S}_i - [\mathrm{k}_{2(i)} + \mathrm{k}_{3(i)}]C_i, \tag{21b}$$

$$\frac{\mathrm{d}[{}^{d_h}_{c_h}P_h^{\gamma_h}]}{\mathrm{d}t} = \sum_i u_{\gamma_{hi}} y_{d_{hi}} \mathrm{k}_{3(i)} C_i. \tag{21c}$$

$$\frac{\mathrm{d}E}{\mathrm{d}t} = -\sum_i \frac{\mathrm{d}C_i}{\mathrm{d}t}, \tag{21d}$$

with $E(t) = E_o - \sum C_i(t)$ in Eqs. (21a) and (21b). Equation (21d) states that the rate of change of the free enzyme concentration depends only on the rate of change of total complex concentration. The isotopic ratios and fractionation factor can be written following Eqs. (11), Eq. (14), and Eq. (15)

### 4.2. Quasi-Steady-State (QSS) treatment

The quasi-steady-state (QSS) treatment of chemical kinetics, originally proposed as the Haldane-Briggs assumption [Haldane, 1930; Laidler, 1965], assumes that complexation of $C_i$ is very fast during the early stage of the reactions, and that, afterwards, $C_i$ does not appreciably change in time. This assumption implies that, after the initial phase,

$$\frac{\mathrm{d}C_i}{\mathrm{d}t} \simeq 0 \qquad \text{and} \qquad \frac{\mathrm{d}E}{\mathrm{d}t} \simeq 0, \tag{22}$$

from the mass conservation law in Eq. (20).

We apply here the quasi-steady-state assumption to the BFEI treatment of Section 4.1. Taking into account that the free enzyme concentration is a function of each complex, $C_i$, as stated in the mass conservation law of Eq. (20), we can write the rate of change of each complex as

$$\frac{\mathrm{d}C_i}{\mathrm{d}t} = \mathrm{k}_{1(i)} \left( E_0 - \sum_{p=1}^{m} C_p \right) \overline{S}_i - [\mathrm{k}_{2(i)} + \mathrm{k}_{3(i)}] C_i \simeq 0,$$

which leads to

$$C_i \simeq \frac{E_0 \overline{S}_i}{\overline{S}_i + K_i \left( 1 + \sum_{p \neq i} \frac{\overline{S}_p}{K_p} \right)}, \tag{23}$$

where $K_i = [\mathrm{k}_{2(i)} + \mathrm{k}_{3(i)}]/\mathrm{k}_{1(i)}$ is equivalent to the Michaelis-Menten constant for the $i$th reaction, and $\overline{S}_i$ is the most limiting reactant in the same reaction.

Using the quasi-steady-state assumption of Eq. (22) and the solution for the complexes $C_i$ of Eq. (23) we can write approximate GEBIK equations that also include the BFEI and QSS assumptions as

$$\frac{\mathrm{d}[{}^{b_j}_{a_j} S_j^{\beta_j}]}{\mathrm{d}t} \simeq - \sum_{i=1}^{m} \frac{x_{b_{ji}} \mathrm{k}_{3(i)} E_0 \overline{S}_i}{\overline{S}_i + K_i \left( 1 + \sum_{p \neq i} \frac{\overline{S}_p}{K_p} \right)}, \tag{24a}$$

$$\frac{\mathrm{d}[{}^{d_h}_{c_h} P_h^{\gamma_h}]}{\mathrm{d}t} \simeq \sum_{i=1}^{m} \frac{u_{\gamma_{hi}} y_{d_{hi}} \mathrm{k}_{3(i)} E_0 \overline{S}_i}{\overline{S}_i + K_i \left( 1 + \sum_{p \neq i} \frac{\overline{S}_p}{K_p} \right)}. \tag{24b}$$

The instantaneous isotopic ratio of product, $IR_P(t)$, and substrate, $R_S(t)$, can be calculated using the above kinetic equations. Next, these ratios can be used to calculate the fractionation factor $\alpha$ defined in Section 3.2.

## 5. Isotopic effects

The GEBIK equations are used to define the instantaneous cumulative isotopic ratio, $IR_P$, and the fractionation factor, $\alpha$. Consequently, the BFEI and QSS approximations of GEBIK have important consequences on how the isotopic effects are described in GEBIF,

and introduce characteristics which are analyzed in this section by means of simple examples.

When the full GEBIK equations are used, the fractionation factor $\alpha$ calculated using the GEBIF equations is always expressed as a nonlinear combination of the substrate and complex concentrations (see *Example 4* and *Example 5* in which S and C appear both at numerator and denominator). Because substrates and complexes are time varying, the fractionation factor $\alpha$ is a function of time and not necessarily constant. When the BFEI and QSS assumptions are used to solve the GEBIK equations, the isotopic effects in GEBIF do not depend on the complex concentrations. In this instance, two scenarios are possible depending on the reaction structure. If more than one isotopologue expression of the same substrate is present in one or more reactions, the isotopic effects are always nonlinear combinations of the substrate concentrations, that is, $\alpha$ is again a function of time. This feature is shown below in *Example 6*, in which the isotope tracer appears with two expressions in the second reaction (i.e., in reactants ${}^0_1S(t)$ and ${}^1_1S(t)$). Conversely, if only one isotopic expression is present in each reaction, then the isotopic effects are always constant, that is, $\alpha$ is strictly a function of the rate constants and it does not depend on the substrate concentration or time. This characteristic is shown in *Example 7*, in which each reaction comprises exclusively one isotopologue expression of the same reactant, i.e., only ${}^0_1S(t)$ in reaction $i = 1$ and only ${}^1_1S(t)$ in reaction $i = 3$.

The full GEBIK and GEBIF equations demonstrate that the isotopic effects (fractionation and enrichment) are a function of time. When a biochemical reaction can be described with the BFEI and QSS approximations of GEBIK and GEBIF, the isotopic effects are either time changing or constant depending on the structure of the reaction. The GEBIK

and GEBIF equations, regardless of whether they are solved under the full treatment or the BFEI-QSS approximations, show an additional important property. Normally, if corresponding rate constants in $m$ isotopologue reactions have identical values, the $m$ reactions are assumed not to produce fractionation and, therefore, the value of the fractionation factor is expected to be $\alpha = 1$. In contrast, our mathematical approach shows that a reaction that does not lead to fractionation may have $\alpha \neq 1$. We demonstrate this property in *Example 8*.

- *Example 6.* Consider the reactions in Eqs. (6) of *Example 1*

$$
\begin{aligned}
2\,{}^{0}_{1}\mathrm{S} \quad + \mathrm{E} &\underset{\mathrm{k}_{2(1)}}{\overset{\mathrm{k}_{1(1)}}{\rightleftarrows}} \mathrm{C}_1 \xrightarrow{\mathrm{k}_{3(1)}} {}^{0}_{2}\mathrm{P} + \mathrm{E},\\
{}^{0}_{1}\mathrm{S} + {}^{1}_{1}\mathrm{S} + \mathrm{E} &\underset{\mathrm{k}_{2(2)}}{\overset{\mathrm{k}_{1(2)}}{\rightleftarrows}} \mathrm{C}_2 \xrightarrow{\mathrm{k}_{3(2)}} u_{\beta}\,{}^{1}_{2}\mathrm{P}^{\beta} + u_{\gamma}\,{}^{1}_{2}\mathrm{P}^{\gamma} + \mathrm{E},\\
2\,{}^{1}_{1}\mathrm{S} + \mathrm{E} &\underset{\mathrm{k}_{2(3)}}{\overset{\mathrm{k}_{1(3)}}{\rightleftarrows}} \mathrm{C}_3 \xrightarrow{\mathrm{k}_{3(3)}} {}^{2}_{2}\mathrm{P} + \mathrm{E},
\end{aligned}
$$

Under the BFEI and QSS assumptions, the GEBIK and GEBIF equations become

$$
\begin{aligned}
\frac{\mathrm{d}[{}^0_2P]}{\mathrm{d}t} &\simeq \frac{\mathrm{k}_{3(1)}E_{0}{}^0_1S}{{}^0_1S + K_1\left(1+\frac{{}^1_1S}{K_2}+\frac{{}^1_1S}{K_3}\right)},\\
\frac{\mathrm{d}[{}^1_2P^\beta]}{\mathrm{d}t} &\simeq \frac{u_\beta \mathrm{k}_{3(2)}E_{0}{}^1_1S}{{}^1_1S + K_2\left(1+\frac{{}^1_0S}{K_1}+\frac{{}^1_1S}{K_3}\right)},\\
\frac{\mathrm{d}[{}^1_2P^\gamma]}{\mathrm{d}t} &\simeq \frac{(1-u_\beta)}{u_\beta}\frac{\mathrm{d}[{}^1_2P^\beta]}{\mathrm{d}t},\\
\frac{\mathrm{d}[{}^2_2P]}{\mathrm{d}t} &\simeq \frac{\mathrm{k}_{3(3)}E_{0}{}^1_1S}{{}^1_1S + K_3\left(1+\frac{{}^1_0S}{K_1}+\frac{{}^1_1S}{K_2}\right)},\\
R_S(t) &= \frac{15/63\ {}^1_1S(t)}{14/62\ {}^0_1S(t)},\\
IR_P(t) &= \frac{330}{161}\frac{[23\ \mathrm{k}_{3(2)}K_3 + 45\ \mathrm{k}_{3(3)}K_2]^1_1S(t)}{45\ \mathrm{k}_{3(1)}K_2{}^0_1S(t) + 44\ \mathrm{k}_{3(2)}K_1{}^1_1S(t)},\\
\alpha(t) &= \frac{1386}{713}\frac{[23\ \mathrm{k}_{3(2)}K_3 + 45\ \mathrm{k}_{3(3)}K_2]^0_1S(t)}{45\ \mathrm{k}_{3(1)}K_2{}^0_1S(t) + 44\ \mathrm{k}_{3(2)}K_1{}^1_1S(t)}.
\end{aligned}
\tag{26}
$$

Equation (26) shows that, in this case, $\alpha$ is not a function of the complex concentrations in contrast to the results shown in *Examples 4* and *Example 5*. However, $\alpha$ is a function of time because reactants ${}^0_1S(t)$ and ${}^1_1S(t)$ appear in more than one reaction.

- *Example 7.* Take again the system in *Example 6* but consider only the first and the third reactions, that is, the rate constants $\mathrm{k}_{1(2)} = \mathrm{k}_{2(2)} = \mathrm{k}_{3(2)} = 0$

$$
\begin{aligned}
2^0_1\mathrm{S} + \mathrm{E} &\underset{\mathrm{k}_{2(1)}}{\overset{\mathrm{k}_{1(1)}}{\rightleftarrows}} \mathrm{C}_1 \xrightarrow{\mathrm{k}_{3(1)}} {}^0_2\mathrm{P} + \mathrm{E},\\
2^1_1\mathrm{S} + \mathrm{E} &\underset{\mathrm{k}_{2(3)}}{\overset{\mathrm{k}_{1(3)}}{\rightleftarrows}} \mathrm{C}_3 \xrightarrow{\mathrm{k}_{3(3)}} {}^2_2\mathrm{P} + \mathrm{E}.
\end{aligned}
$$

The GEBIK and GEBIF equations written under the BFEI and QSS assumptions become

$$
\begin{aligned}
\frac{\mathrm{d}[{}^0_2P]}{\mathrm{d}t} &\simeq \frac{\mathrm{k}_{3(1)} E_{01} {}^0_1S}{{}^0_1S + K_1\left(1 + \frac{{}^1_1S}{K_3}\right)}, \\
\frac{\mathrm{d}[{}^2_2P]}{\mathrm{d}t} &\simeq \frac{\mathrm{k}_{3(3)} E_{01} {}^1_1S}{{}^1_1S + K_3\left(1 + \frac{{}^0_1S}{K_1}\right)}, \\
R_S(t) &= \frac{15/63\ {}^1_1S(t)}{14/62\ {}^0_1S(t)}, \\
IR_P(t) &= \frac{330}{161}\frac{\mathrm{k}_{3(3)} K_1 {}^1_1S}{\mathrm{k}_{3(1)} K_3 {}^0_1S}, \\
\alpha &= \frac{1386}{713}\frac{\mathrm{k}_{3(3)} K_1}{\mathrm{k}_{3(1)} K_3}.
\end{aligned}
\tag{28}
$$

Notice that the fractionation factor of Eq. (28) does not depend on the substrate concentration but is constant over time in contrast to *Example 6*.

• *Example 8.* Consider the fractionation factor derived using the full GEBIK and GEBIF as in *Example 4* and *Example 5*. Assuming that the rate constants $\mathrm{k}_3$ have the same value in the three reactions, the fractionation factors can be calculated as

$$
\alpha(t) = \frac{693}{713}\frac{[23C_2(t) + 45\ C_3(t)]}{[45C_1(t) + 22C_2(t)]}\frac{{}^0_1S(t)}{{}^1_1S(t)}, \tag{29}
$$

$$
\alpha(t) = \frac{693}{713}\frac{C_3(t)}{C_1(t)}\frac{{}^0_1S(t)}{{}^1_1S(t)}. \tag{30}
$$

In both reaction schemes $\alpha$ is a function of time and not necessarily equal to 1. Similarly, consider the fractionation factor derived from GEBIK and GEBIF under the BFEI-QSS approximations of *Example 6* and *Example 7*; assume the rate constant $\mathrm{k}_3$ have the same value in the corresponding reactions, and the Michaelis-Menten equivalent concentrations

are $K_1 = K_2 = K_3$. Under these constraints, the fractionation factors become, for *Example 6* and *Example 7*, respectively

$$\alpha(t) = \frac{1386}{713} \frac{[23+45]\ {}^{0}_{1}S(t)}{45\ {}^{0}_{1}S(t) + 44\ {}^{1}_{1}S(t)}, \tag{31}$$

$$\alpha = \frac{1386}{713}. \tag{32}$$

It is clear that $\alpha$ is not necessarily equal to 1 when corresponding rate constants have identical values in $m$ isotopologue reactions, that is, when reactants identically react in each reaction regardless of the isotopic expressions. However, depending on the reaction structure, $\alpha$ may either be time-varying or constant as shown above.

## 6. Application of GEBIK and GEBIF to denitrification

In this section we describe the application of the full GEBIK and GEBIF equations and their approximations solved under the BFEI and QSS assumptions to describe the denitrification reactions of $N_2O$ production and consumption. To this end, the experimental observations in soil samples by Menyailo and Hungate [2006] and Mariotti *et al.* [1981] provide the necessary constraints to the model and, at the same time, show non-common inverse isotopic effects (i.e., $N_2O$ consumption in Menyailo and Hungate [2006]). Similar inverse effects were observed for $^{18}O$ during $N_2O$ production [Toyoda *et al.*, 2005], during $N_2$ fixation [Yamazaki *et al.*, 1987], and during intermediate $NO_2^- \rightarrow N_2O$ in-cell redox reactions [Shearer and Kohl, 1988]. However, the data density in these experiments could not be used to constrain the parameters involved in the GEBIK and GEBIF presented here. The use of Manyailo and Hungate's and Mariotti's and co-worker experiments is aimed to illustrate the main features of the two forms of GEBIK and GEBIF presented

in Section 2, 3 and 4, whereas a detailed interpretation of the experiments can be found in Menyailo and Hungate [2006] and in Maggi and Riley [2009].

### 6.1. Experimental data

The experimental data used in this application were collected from incubated soils tests of $N_2O$ production from $NO_3^-$ [Mariotti *et al.*, 1981; Menyailo and Hungate, 2006], and $N_2O$ consumption into $N_2$ [Menyailo and Hungate, 2006]. In both experiments, the bulk $\delta^{15}$N-$NO_3^-$ and $\delta^{15}$N-$N_2O$ were measured during $N_2O$ production using $N_2O$-reductase acetylene inhibition. The $\delta^{15}$N-$N_2O$ were measured with no additional treatment during $N_2O$ consumption. During $N_2O$ production, the isotopomer speciation of the asymmetric molecules $^{15}N^{14}NO$ and $^{14}N^{15}NO$ were not assessed. However, in a similar experiment of $N_2O$ production from $NO_3^-$, [Well *et al.*, 2006] measured the signature of the two isotopomers in soils treated with moisture saturation ranging from 0.55 to 0.85. Their analysis showed that the average isotopomer speciation was 50.225% as $^{14}N^{15}NO$ and 49.775% as $^{15}N^{14}NO$ with a very small standard deviation across the water saturation treatments. We will use these values for the partitioning coefficients introduced in the GEBIK and GEBIF equations.

The numerical solution of the kinetics of each system component was obtained with an explicit finite difference technique. Model calibration was carried out using $N_2O$ concentration and $\delta^{15}$N measured in both $N_2O$ production and consumption tests. For these applications, the enzyme yield coefficient was arbitrarily set at $z = 0.01$ knowing that the ratio $E/B$ is small, while the microbial death rate was set at $\mu = 10^{-6}$ s$^{-1}$ knowing that it ranges between $10^{-7}$ s$^{-1}$ and 1.15 $10^{-6}$ s$^{-1}$ [e.g., Salem *et al.*, 2005; Kim, 2006]. The enzyme yield coefficient and the mortality rate were held identical in the $N_2O$ production

and consumption tests assuming that there is only one function group of denitrifying bacteria in these tests. The remaining parameters (highlighted in brackets in the first column) were obtained by calibration using the software package PEST (Parameter ESTimation, Papadopulos & Associates Inc., www.sspa.com/pest). Table 1 summarizes the parameters used and calibrated for these experiments. Calibration of the rate constants was carried out in a way such to satisfy the conditions $k_{1(1)} \geq k_{1(2)}$, $k_{2(1)} \geq k_{2(2)}$, and $k_{3(1)} \geq k_{3(2)}$ in the full GEBIK equations, and the condition $k_{3(1)} \geq k_{3(2)}$ in the GEBIK equations solved under BFEI and QSS assumptions. These conditions were imposed on the basis of the higher energy barrier required in reactions involving molecules with heavier isotopes.

### 6.2. $N_2O$ production

$N_2O$ production from $NO_3^-$ can be described by the reactions

$$2\,{}^{0}_{1}\mathrm{S} + \mathrm{E} \underset{k_{2(1)}}{\overset{k_{1(1)}}{\rightleftarrows}} \mathrm{C}_1 \xrightarrow{k_{3(1)}} {}^{0}_{2}\mathrm{P} + \mathrm{E},$$

$$ {}^{0}_{1}\mathrm{S} + {}^{1}_{1}\mathrm{S} + \mathrm{E} \underset{k_{2(2)}}{\overset{k_{1(2)}}{\rightleftarrows}} \mathrm{C}_2 \xrightarrow{k_{3(2)}} u_\beta\, {}^{1}_{2}\mathrm{P}^{\beta} + u_\gamma\, {}^{1}_{2}\mathrm{P}^{\gamma} + \mathrm{E},$$

where production of ${}^{2}_{2}\mathrm{P} = {}^{15}\mathrm{N_2O}$ from ${}^{1}_{1}\mathrm{S} = {}^{15}\mathrm{NO_3^-}$ was excluded due to its scarcity. The isotopomer partitioning coefficients $u_\beta = 0.5022$ and $u_\gamma = 1 - u_\beta = 0.4978$ were derived from the experiments presented in Well *et al.* [2006]. The full GEBIK and GEBIF equations describing $N_2O$ production are

$$\frac{\mathrm{d}[{}^{0}_{1}S]}{\mathrm{d}t} = 2[\mathrm{k}_{2(1)}C_1 - \mathrm{k}_{1(1)}{}^{0}_{1}SE] + \frac{\mathrm{d}[{}^{1}_{1}S]}{\mathrm{d}t}, \tag{34a}$$

$$\frac{\mathrm{d}[{}^{1}_{1}S]}{\mathrm{d}t} = \mathrm{k}_{2(2)}C_2 - \mathrm{k}_{1(2)}{}^{1}_{1}SE, \tag{34b}$$

$$\frac{\mathrm{d}C_1}{\mathrm{d}t} = \mathrm{k}_{1(1)}{}^{0}_{1}SE - (\mathrm{k}_{2(1)} + \mathrm{k}_{3(1)})C_1, \tag{34c}$$

$$\frac{\mathrm{d}C_2}{\mathrm{d}t} = \mathrm{k}_{1(2)}{}^{1}_{1}SE - (\mathrm{k}_{2(2)} + \mathrm{k}_{3(2)})C_2, \tag{34d}$$

$$\frac{\mathrm{d}[{}^{0}_{2}P]}{\mathrm{d}t} = \mathrm{k}_{3(1)}C_1, \tag{34e}$$

$$\frac{\mathrm{d}[{}^{1}_{2}P^{\beta}]}{\mathrm{d}t} = u_\beta \mathrm{k}_{3(2)}C_2, \tag{34f}$$

$$\frac{\mathrm{d}[{}^{1}_{2}P^{\gamma}]}{\mathrm{d}t} = \frac{1-u_\beta}{u_\beta}\frac{\mathrm{d}[{}^{1}_{2}P^{\beta}]}{\mathrm{d}t}, \tag{34g}$$

$$\frac{\mathrm{d}E}{\mathrm{d}t} = z\frac{\mathrm{d}B}{\mathrm{d}t} - \frac{\mathrm{d}C_1}{\mathrm{d}t} - \frac{\mathrm{d}C_2}{\mathrm{d}t}, \tag{34h}$$

$$\frac{\mathrm{d}B}{\mathrm{d}t} = Y\left(\frac{\mathrm{d}[{}^{0}_{2}P]}{\mathrm{d}t} + \frac{\mathrm{d}[{}^{1}_{2}P^{\beta}]}{\mathrm{d}t} + \frac{\mathrm{d}[{}^{1}_{2}P^{\gamma}]}{\mathrm{d}t}\right) - \mu B, \tag{34i}$$

$$R_P(t) = \frac{165\ {}^{1}_{2}P}{154\ {}^{1}_{2}P + 315\ {}^{0}_{2}P}, \tag{34j}$$

$$IR_P(t) = \frac{165\ \mathrm{k}_{3(2)}C_2}{154\ \mathrm{k}_{3(2)}C_2 + 315\ \mathrm{k}_{3(1)}C_1}, \tag{34k}$$

$$R_S(t) = \frac{155}{147}\frac{{}^{1}_{1}S}{{}^{0}_{1}S}, \tag{34l}$$

$$\alpha(t) = \frac{693\ \mathrm{k}_{3(2)}C_2}{1395\ \mathrm{k}_{3(1)}C_1 + 682\ \mathrm{k}_{3(2)}C_2}\frac{{}^{0}_{1}S}{{}^{1}_{1}S}, \tag{34m}$$

with ${}^{1}_{2}P(t) = {}^{1}_{2}P^{\beta}(t) + {}^{1}_{2}P^{\gamma}(t)$ in Eq. (34j).

For the same system, the GEBIK and GEBIF equations under the BFEI and QSS approximations are

$$\frac{\mathrm{d}[{}^0_1S]}{\mathrm{d}t} = -2\frac{\mathrm{d}[{}^0_2P]}{\mathrm{d}t} - \frac{1}{u_\beta}\frac{\mathrm{d}[{}^1_2P^\beta]}{\mathrm{d}t}, \tag{35a}$$

$$\frac{\mathrm{d}[{}^1_1S]}{\mathrm{d}t} = -\frac{1}{u_\beta}\frac{\mathrm{d}[{}^1_2P^\beta]}{\mathrm{d}t}, \tag{35b}$$

$$\frac{\mathrm{d}[{}^0_2P]}{\mathrm{d}t} \simeq \frac{\mathrm{k}_{3(1)}E_0{}^0_1S}{{}^0_1S + K_1\left(1 + \frac{{}^1_1S}{K_2}\right)}, \tag{35c}$$

$$\frac{\mathrm{d}[{}^1_2P^\beta]}{\mathrm{d}t} \simeq \frac{u_\beta \mathrm{k}_{3(2)}E_0{}^1_1S}{{}^1_1S + K_2\left(1 + \frac{{}^1_0S}{K_1}\right)}, \tag{35d}$$

$$\frac{\mathrm{d}[{}^1_2P^\gamma]}{\mathrm{d}t} \simeq \frac{1-u_\beta}{u_\beta}\frac{\mathrm{d}[{}^0_2P^\beta]}{\mathrm{d}t}, \tag{35e}$$

$$IR_P(t) = \frac{165\ \mathrm{k}_{3(2)}K_1{}^1_1S}{315\ \mathrm{k}_{3(1)}K_2{}^0_1S + 154\ \mathrm{k}_{3(2)}K_1{}^1_1S}, \tag{35f}$$

$$\alpha(t) = \frac{693\ \mathrm{k}_{3(2)}K_1{}^0_1S}{1395\ \mathrm{k}_{3(1)}K_2{}^0_1S + 682\ \mathrm{k}_{3(2)}K_1{}^1_1S}. \tag{35g}$$

Relatively to the experiments by Menyailo and Hungate [2006], $N_2O$ product concentrations and $\delta^{15}N$ values predicted from the full and approximate forms of the GEBIK and GEBIF equations are relatively similar (Figure (1a) and (1b)). The fractionation factor (Figure 1c) is not constant in both forms of GEBIF owing to the mixed reaction in which ${}^0_1S$ and ${}^1_1S$ produce the isotopomers ${}^1_2P^\beta$ and ${}^1_2P^\gamma$. Notice that the Michaelis-Menten constants $K_1$ approximate well 4.5 mmol $NO_3^-$ $kg_{soil}^{-1}$ reported in Li *et al.* [1992] (Table 1). The values of $K_2$, smaller by about 2 mmol $NO_3^-$ $kg_{soil}^{-1}$, may reflect differences in experimental setup. Interestingly, the $K_1$ and $K_2$ values obtained by calibration of the BFEI-QSS approximation of GEBIK and GEBIF are very similar to the values calculated a posteriori with the rated constants of the full GEBIK and GEBIF.

The full and approximate forms of the GEBIK and GEBIF applied to the experimental data from Mariotti *et al.* [1981] predict very well the concentrations of $N_2O$ and $NO_3^-$ and $\delta^{15}N$ (Figure 2). In this case, the full GEBIK and GEBIF approach performs better than

the approximate forms, but the differences in accuracy are relatively small. It is important to observe that the values of rate constants obtained by calibration on this experiment have very similar values to those obtained from data by Menyailo and Hungate [2006], thus signifying that the model can capture the reaction kinetics consistently.

As evidenced in Figure 1*c* and 2*c*, the fractionation factor $\alpha$ is time varying in both full and approximate forms of GEBIK and GEBIF.

### 6.3. $N_2O$ consumption

$N_2O$ consumption can be described by the following reactions

$$
\begin{aligned}
{}^{14}\mathrm{N_2O} &\rightarrow {}^{14}\mathrm{N_2},\\
{}^{14}\mathrm{N^{15}NO} &\rightarrow {}^{14}\mathrm{N^{15}N},\\
{}^{15}\mathrm{N^{14}NO} &\rightarrow {}^{14}\mathrm{N^{15}N},
\end{aligned}
$$

which can be rewritten using the generalized notation in Eqs. (4) as

$$
{}^{0}_{2}\mathrm{S} + \mathrm{E} \underset{\mathrm{k}_{2(1)}}{\overset{\mathrm{k}_{1(1)}}{\rightleftarrows}} \mathrm{C}_1 \overset{\mathrm{k}_{3(1)}}{\rightarrow} {}^{0}_{2}\mathrm{P} + \mathrm{E}, \tag{37a}
$$

$$
{}^{1}_{2}\mathrm{S}^{\beta} + \mathrm{E} \underset{\mathrm{k}_{2(2)}}{\overset{\mathrm{k}_{1(2)}}{\rightleftarrows}} \mathrm{C}_2 \overset{\mathrm{k}_{3(2)}}{\rightarrow} {}^{1}_{2}\mathrm{P} + \mathrm{E}, \tag{37b}
$$

$$
{}^{1}_{2}\mathrm{S}^{\gamma} + \mathrm{E} \underset{\mathrm{k}_{2(3)}}{\overset{\mathrm{k}_{1(3)}}{\rightleftarrows}} \mathrm{C}_3 \overset{\mathrm{k}_{3(3)}}{\rightarrow} {}^{1}_{2}\mathrm{P} + \mathrm{E}, \tag{37c}
$$

where ${}^{0}_{2}\mathrm{S} = {}^{14}\mathrm{N_2O}$, ${}^{1}_{2}\mathrm{S}^{\beta} = {}^{14}\mathrm{N^{15}NO}$, ${}^{1}_{2}\mathrm{S}^{\gamma} = {}^{15}\mathrm{N^{14}NO}$, ${}^{0}_{2}\mathrm{P} = \mathrm{N_2}$, and ${}^{1}_{2}\mathrm{P} = {}^{15}\mathrm{N^{14}N}$. Here, we have not considered the substrate ${}^{2}_{2}\mathrm{S} = {}^{15}\mathrm{N_2O}$ due to its scarcity. In addition, we have not specified the isotopic substitution in the $N_2$ product of the second and third reactions because $N_2$ is symmetric.

Assuming that the second and third reactions in Eqs. (37b) and (37c) have identical reaction rates ($k_{1(3)} \equiv k_{1(2)}$, $k_{2(3)} \equiv k_{2(2)}$, and $k_{3(3)} \equiv k_{3(2)}$), the full GEBIK and GEBIF equations describing the reactions in Eqs. (37) are

$$\frac{d[{}^0_2 S]}{dt} = k_{2(1)} C_1 - k_{1(1)} {}^0_2 S E, \tag{38a}$$

$$\frac{d[{}^1_2 S^\beta]}{dt} = k_{2(2)} C_2 - k_{1(2)} {}^1_2 S^\beta E, \tag{38b}$$

$$\frac{d[{}^1_2 S^\gamma]}{dt} = k_{2(2)} C_3 - k_{1(2)} {}^1_2 S^\gamma E, \tag{38c}$$

$$\frac{dC_1}{dt} = k_{1(1)} {}^0_2 S E - (k_{2(1)} + k_{3(1)}) C_1, \tag{38d}$$

$$\frac{dC_2}{dt} = k_{1(2)} {}^1_2 S^\beta E - (k_{2(2)} + k_{3(2)}) C_2, \tag{38e}$$

$$\frac{dC_3}{dt} = k_{1(2)} {}^1_2 S^\gamma E - (k_{2(2)} + k_{3(2)}) C_3, \tag{38f}$$

$$\frac{d[{}^0_2 P]}{dt} = k_{3(1)} C_1, \tag{38g}$$

$$\frac{d[{}^1_2 P]}{dt} = k_{3(2)} (C_2 + C_3), \tag{38h}$$

$$\frac{dE}{dt} = z \frac{dB}{dt} - \frac{dC_1}{dt} - \frac{dC_2}{dt} - \frac{dC_3}{dt}, \tag{38i}$$

$$\frac{dB}{dt} = Y \left( \frac{d[{}^0_2 P]}{dt} + \frac{d[{}^1_2 P]}{dt} \right) - \mu B, \tag{38j}$$

$$R_P(t) = \frac{15 \; {}^1_2 P(t)}{14 \; {}^1_2 P(t) + 29 \; {}^0_2 P(t)}, \tag{38k}$$

$$IR_P(t) = \frac{15 \; (C_2 + C_3) k_{3(2)}}{29 \; C_1 k_{3(1)} + 14 \; (C_2 + C_3) k_{3(2)}},$$

$$R_S(t) = \frac{165 \; {}^1_2 S}{154 \; {}^1_2 S + 315 \; {}^0_2 S}, \tag{38l}$$

$$\alpha(t) = \frac{7 \; (C_2 + C_3) k_{3(2)} [45 \; {}^0_2 S + 22 \; {}^1_2 S]}{11 \; [29 \; C_1 k_{3(1)} + 14 \; (C_2 + C_3) k_{3(2)}] \; {}^1_2 S}. \tag{38m}$$

The same equations with the BFEI and QSS approximations are

$$\frac{\mathrm{d}[{}^0_2S]}{\mathrm{d}t} \simeq -\frac{\mathrm{k}_{3(1)}E_{02}{}^0_2S}{{}^0_2S + K_1\left(1 + \frac{{}^1_2S^\beta}{K_2} + \frac{{}^1_2S^\gamma}{K_2}\right)}, \tag{39a}$$

$$\frac{\mathrm{d}[{}^1_2S^\beta]}{\mathrm{d}t} \simeq -\frac{\mathrm{k}_{3(2)}E_{02}{}^1_2S^\beta}{{}^1_2S^\beta + K_2\left(1 + \frac{{}^0_2S}{K_1} + \frac{{}^1_2S^\gamma}{K_2}\right)}, \tag{39b}$$

$$\frac{\mathrm{d}[{}^1_2S^\gamma]}{\mathrm{d}t} \simeq -\frac{\mathrm{k}_{3(2)}E_{02}{}^1_2S^\gamma}{{}^1_2S^\gamma + K_2\left(1 + \frac{{}^0_2S}{K_1} + \frac{{}^1_2S^\beta}{K_2}\right)}, \tag{39c}$$

$$\frac{\mathrm{d}\ {}^0_2P}{\mathrm{d}t} = -\frac{\mathrm{d}[{}^0_2S]}{\mathrm{d}t}, \tag{39d}$$

$$\frac{\mathrm{d}\ {}^1_2P}{\mathrm{d}t} = -\frac{\mathrm{d}[{}^1_2S^\beta]}{\mathrm{d}t} - \frac{\mathrm{d}[{}^1_2S^\gamma]}{\mathrm{d}t}, \tag{39e}$$

$$R_P(t) = \frac{15{}^1_2P}{14{}^1_2P + 29\ {}^0_2P}, \tag{39f}$$

$$IR_P(t) = \frac{15K_1\mathrm{k}_{3(2)}{}^1_2S}{29K_2\mathrm{k}_{3(1)}{}^0_2S + 14K_1\mathrm{k}_{3(2)}{}^1_2S}, \tag{39g}$$

$$R_S(t) = \frac{465\ {}^1_2S}{14[63\ {}^0_2S + 31\ {}^1_2S]}, \tag{39h}$$

$$\alpha(t) = \frac{14K_1\mathrm{k}_{3(2)}[63\ {}^0_2S + 31\ {}^1_2S]}{31[29K_2\mathrm{k}_{3(1)}\ {}^0_2S + 14K_1\mathrm{k}_{3(2)}\ {}^0_2S]}, \tag{39i}$$

where $K_3$ has been substituted with $K_2$ because the rate constants in the third reaction have been assumed to equal those of the second reaction. In addition, ${}^1_2S = {}^1_2S^\beta + {}^1_2S^\gamma$ has been taken in Eqs. (39g), (39h), and (39i).

The full GEBIK and GEBIF equations capture the $N_2O$ and $\delta^{15}N$ values with higher accuracy as compared to the GEBIK and GEBIF equations solved under the BFEI and QSS approximations (Figure 3a and Figure 3b). Also in this case the fractionation factor is not constant, as shown in Eqs. (38m) and (39i). The variability of $\alpha$ obtained from the GEBIF equations solved under BFEI and QSS is small as compared to that obtained from the full solution of GEBIK and GEBIF (see insert in Figure (3c)), but has a strong impact on the curvature of $\delta^{15}N$ in Figure (3b). Also in this case, we observe that $K_1$

and $K_2$ values calculated a posteriori with the full GEBIK and GEBIF are very similar to those calibrated under the QSS and BFEI approximations, and differ only slightly from values reported in the literature [e.g., Li *et al.*, 1992].

With respect to the specific interpretation of the $N_2O$ consumption experiment, it is important to notice the capability of the full GEBIK and GEBIF equations to predict inverse isotopic effects that result in $\mathrm{d}[\delta^{15}\mathrm{N}]/\mathrm{d}t < 0$ after $t = 80$ h (Figure 3b). Inverse isotopic effects arose when the substrate was almost completely consumed and converted into complex. From around time $t = 90$ h, the small amounts of the complex being transformed back into the substrate controlled its isotope signature and led to a signature close to the initial composition. Finally, it is important to notice that inverse isotopic effects in the full GEBIK and GEBIF equations do not necessarily imply $\alpha > 1$ (Figure 3c). This property of GEBIK and GEBIF is a unique consequence of the transient kinetics, that is, complexation was not assumed to be a steady state process.

## 7. Conclusion

We have presented an original mathematical treatment of isotopologues and isotopomer speciation and fractionation that integrates the Michaelis-Menten kinetics with the Monod kinetics for biomass and enzyme dynamics, and that accounts for (1) non-steady complexation; (2) reaction stoichiometry; and (3) number of isotope substitutions and location within the molecule. We have also developed and tested two mathematical simplifications to the full mathematical treatment by introducing the biomass-free and enzyme-invariant assumption, and the quasi-steady-state assumption for the complexation.

The full representation of isotope kinetics presented here produced the most accurate predictions of observed concentrations in denitrification experiments, and showed the

unique capability to predict variable and inverse isotopic effects as compared to previous mathematical approaches. The full GEBIK and GEBIF equations demonstrated that: (*i*) microbial biomass and enzyme dynamics substantially improve modeling of biochemical isotopic kinetics; (*ii*) isotopic effects are always time-dependent because they are linked to the substrate and complex concentrations; (*iii*) inverse isotopic effects can be modeled only assuming transient kinetics, i.e., when the complexation is not assumed in quasi-steady state; (*iv*) inverse isotopic effects may occur also for values of the fractionation factor smaller than 1; and (*v*) a biochemical reaction that does not fractionate isotopes does not necessarily imply a fractionation factor equal to 1, the characteristic which depends on the reaction structure.

More generally, the mathematical treatment presented here suggests that isotopic measurements have the potential to help improve the mathematical understanding of the kinetics of biologically-mediated chemical reactions. However, we recognize that a more comprehensive experimentation into isotopic effects, such as simultaneous measurements of substrate, product, and biomass concentrations, and the components' isotopic composition, is equally important to fully understand the dependence of isotopic effects on otherwise unobservable interactions with non-steady complexes.

## References

Atkins P.W., (1998), *Physical Chemistry*, 6th ed., Freeman, Oxford University Press, pp 999.

Elsner M., L. Zwank, D. Hunkeler and R.P. Schwarzenbach, (2005), A New Concept Linking Observable Stable Isotope Fractionation to Transformation Pathways of Organic

Pollutants, Environ. Sci. Technolo. 39, 6896-6916.

Haldane J.B.S. (1930), *Enzymes*, London, New York, Longmans, Green, pp 235.

Hunkeler D. and R. Aravena (2000), Evidence of Substantial Carbon Isotope Fractionation among Substrate, Inorganic Carbon, and Biomass during Aerobic Mineralization of 1,2-Dichloroethane by Xanthobacter autotrophicus, Applied Environmental Microbiology, 66(11), 4870-4876.

Kim S.-B. (2006), Numerical analysis of bacterial transport in saturated porous media, Hydrological Processes 20, 1177-1186.

Laidler K.J., (1965), *Chemical kinetics*, McGraw-Hill, pp. 566.

Li C., S. Frolking and T.A. Frolking, (1992), A model of Nitrous Oxide Evolution from Soil Driven by Rainfall Events: 1. Model Streucture and Sensitivity, Journal of Geophysical Research 97(D9), 9759-9776.

Mariotti A., J.C. Germon, P. Hubert, P. Kaiser, R. Letolle, A. Tardieux, P. Tardieux, (1981), Experimental determination of nitrogen kinetic isotope fractionation - Some principles - Illustration for the denitrification and nitrification processes, Plant and Soil 62(3), 413-430.

Maggi F. and W.J. Riley, (2009), Transient competitive complexation in biological kinetic isotope fractionation explains non-steady isotopic effects: Theory and application to denitrification in soils, Journal of Geophysical Research - Biogeosciences (in press).

Mauclaire L., Pelza O., Thullner M., Abrahamb W-R. and Zeyer J., (2003), Assimilation of toluene carbon along a bacteriaprotist food chain determined by $^{13}$C-enrichment of biomarker fatty acids, Journal of Microbiological Methods 55, 635-649.

McNaught A.D. and A. Wilkinson, (1997), Compendium of Chemical Terminology, IUPAC Recommendations, The Gold Book, Secon Edition, Blackwell Science, pp. 315.

Menyailo O.V. and B.A. Hungate, (2006), Stable isotope discrimination during soil denitrification: Production and consumption of nitrous oxide, Global Biogeochemical Cycles 20(GB3025), doi:10.1029/2005GB002527.

Monod J., (1949), The growth of bacterial cultures, Annu. Rev. Microbial 3, 371-394.

Northorp D.B., (1980), The expression of isotope effects on enzyme-catalyzed reactions, Annu. Rev. Biochem 50, 103-131.

Perez T., D. GarciaMontiel, S. Trumbore, S. Tyler, P. De Camargo, M. Moreira, M. Piccolo and C. Cerri, (2006), Nitrous oxide nitrification and denitrification $^{15}$n enrichment factors from amazon forest soils

Papadopulos & Associates, Inc., www.sspa.com/pest.

Salem S., Moussa M.S. and van Loosdrecht M.C.M., (2005), Determination of the decay rate of nitrifying bacteria, Biotechnology and Bioengineering, DOI: 10.1002/bit.20822.

Shearer G. and D.H. Kohl, (1988), Nitrogen isotopic fractionation and $^{18}$O exchange in relation to the mechanism of denitrification of nitrite by *Pseudomonas stutzeri*, The Journal of Biological Chemistry 263(26), 13231-13245.

Toyoda S., Mutobe H., Yamagishi H., Yoshida N. and Tanji Y., (2005), Fractionation of $N_2O$ isotopomers during production by denitrifier, Soil Biology and Biogeochemistry 37, 1535-1545.

Thullner M., M. Kamparar, H.H. Richnow, H. Harms and L.Y. Wick, (2008), Impact of Bioavailability Restrictions on Microbially Induced Stable Isotope Fractionation. 1. Theoretical Calculation, Env. Sci. Tech. 42, 6544-6551.

Breukelen Van B.M., D. Hunkeler and F. Volkering, (2005), Quantification of Sequential Chlorinated Ethene Degradation by Use of a Reactive Transport Model Incorporating Isotope Fractionation, Env. Sci. Tech. 39, 4189-4197.

Yamazaki T., N. Yoshida, E. Wada, S. Matsup, (1987), $N_2O$ Reduction by *Azotobacter vinelandii* with Emphasis on Kinetic Nitrogen Isotope Effects, Plant Cell. Physiol 28(2), 263-271.

Well R., I. Kurnegova, V. Lopes de Gerenyu and H. Flessa, (2006), Isotopomer signatures of soil-emitted $N_2O$ under different moisture conditions - A microcosm study with arable loess soil, Soil Biology & Biochemistry 38, 2923-2933.

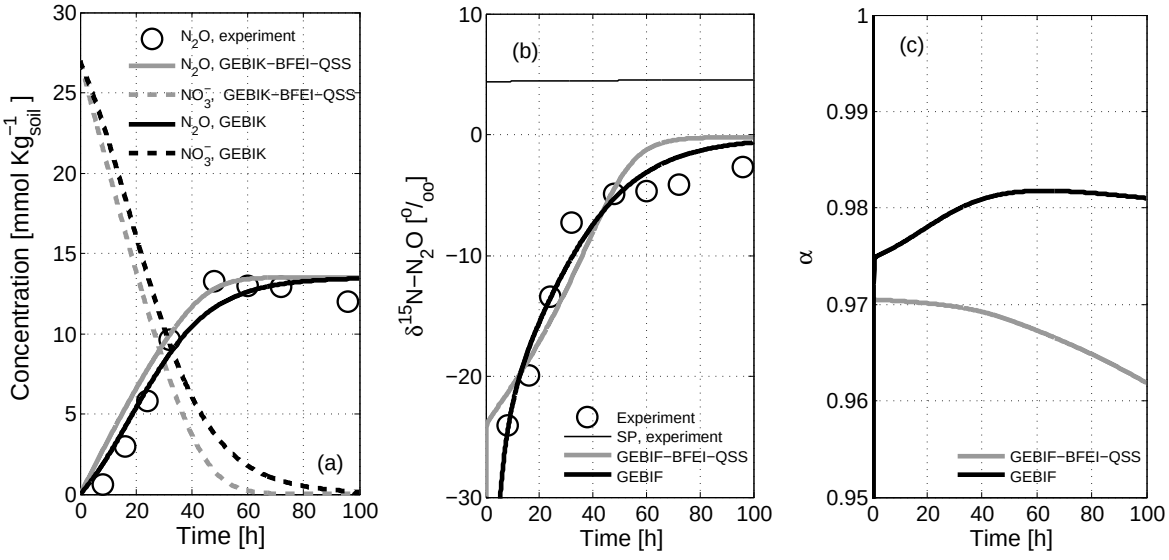


**Figure 1.** ($a$) observed and predicted $N_2O$ concentration, and ($b$) observed and predicted $N_2O$ isotopic composition during $N_2O$ production from $NO_3^-$. ($c$) fractionation factor calculated with the full and BFEI-QSS approximate solutions of GEBIK equations. Experimental data are redrawn from Menyailo and Hungate [2006]. The acronyms BFEI and QSS define, respectively, the biomass-free and enzyme-invariant approximation, and the quasi-steady-state approximation.

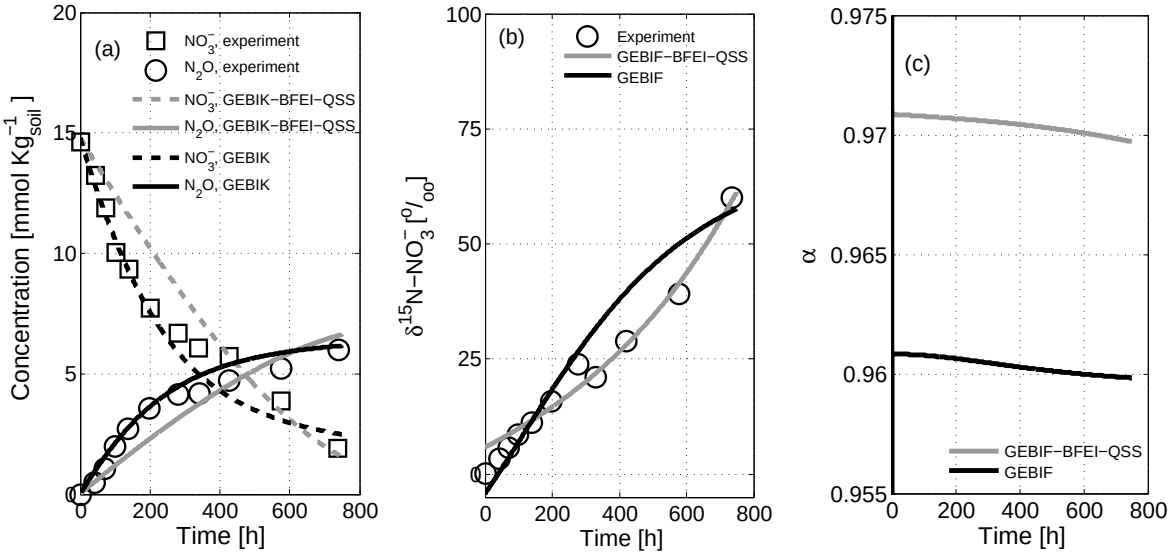


**Figure 2.** (*a*) observed and predicted $N_2O$ concentration, and (*b*) observed and predicted $NO_3^-$ isotopic composition during $N_2O$ production from $NO_3^-$. (*c*) fractionation factor calculated with the full and BFEI-QSS approximate solutions of GEBIK equations. Experimental data are redrawn from Mariotti *et al.* [1981]. The acronyms BFEI and QSS define, respectively, the biomass-free and enzyme-invariant approximation, and the quasi-steady-state approximation.

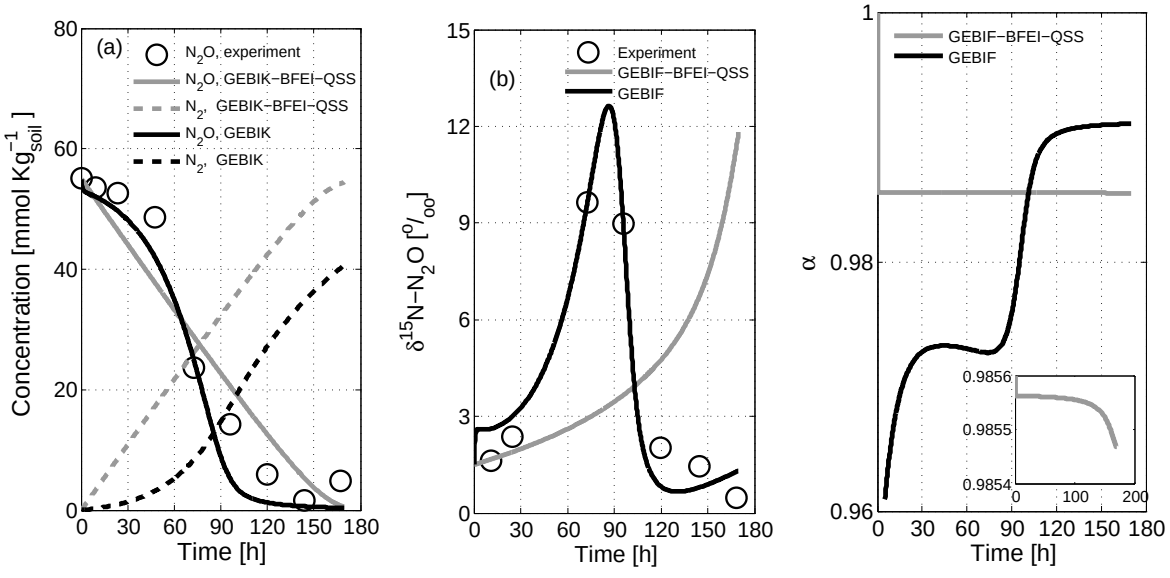


**Figure 3.** ($a$) observed and predicted $N_2O$ concentration, and ($b$) observed and predicted $N_2O$ isotopic composition during $N_2O$ consumption into $N_2$. ($c$) fractionation factor calculated with the full and BFEI-QSS approximate solutions of GEBIK equations. Experimental data are redrawn from Menyailo and Hungate [2006]. The acronyms BFEI and QSS define, respectively, the biomass-free and enzyme-invariant approximation, and the quasi-steady-state approximation.

**Table 1.** Summary of parameters used in the GEBIK and GEBIF equations in the cases of full solution and approximate BFEI-QSS solution for the experiments of $N_2O$ production and consumption from Menyailo and Hungate [2006] (M&H2006) and Mariotti *et al.* [1981] (M1981). The parameters in parentheses in the first column were calibrated, the value $z = 0.01$ was assigned arbitrarily under the assumption that $E/B$ is small, $\mu = 10^{-6}$ s$^{-1}$ was chosen within the range of values reported in Kim [2006] and Salem *et al.* [2005], while $S_0$, $B_0$, and $E_0$ were determined from the experiments. The reference isotopic ratio $R_{std} = 2.305 \cdot 10^{-2}$ was used. The parameters $K_1$ and $K_2$ within *-* in the full solution of GEBIK were calculated a posteriori as $K = (k_2+k_3)/k_1$ for comparison with $K_1$ and $K_2$ of the BFEI-QSS approximate solution of GEBIK. The values of the parameters $k_1(i)$, $k_2(i)$ and $k_3(i)$ are expressed with a precision of four digits owing to the model sensitivity to these values.

| | | | **$N_2O$ production** | | | | **$N_2O$ consumption** | |
|---|---|---|---|---|---|---|---|---|
| Solution of GEBIK | | | Full | | BFEI-QSS | | Full | BFEI-QSS |
| Experiment from | | | M&H2006 | M1981 | M&H2006 | M1981 | M&H2006 | M&H2006 |
| $(k_{1(1)})$ | [mmol$^{-1}$ kg$_{soil}$ s$^{-1}$] | $\cdot 10^{-6}$ | 2.5833 | 2.0872 | - | - | 6.8606 | - |
| $(k_{1(2)})$ | [mmol$^{-1}$ kg$_{soil}$ s$^{-1}$] | $\cdot 10^{-6}$ | 2.5176 | 1.9489 | - | - | 6.6418 | - |
| $(k_{2(1)})$ | [s$^{-1}$] | $\cdot 10^{-6}$ | 9.7848 | 6.3234 | - | - | 15.2727 | - |
| $(k_{2(2)})$ | [s$^{-1}$] | $\cdot 10^{-6}$ | 2.9413 | 1.3275 | - | - | 14.6963 | - |
| $(k_{3(1)})$ | [s$^{-1}$] | $\cdot 10^{-6}$ | 3.3650 | 3.0910 | 4.0319 | 2.5334 | 3.8023 | 3.4542 |
| $(k_{3(2)})$ | [s$^{-1}$] | $\cdot 10^{-6}$ | 3.2914 | 3.0127 | 3.8911 | 2.5294 | 3.7935 | 3.4376 |
| $(K_1)$ | [mmol kg$_{soil}^{-1}$] | | *5.09* | *4.51* | 4.65 | 4.65 | *2.78* | 2.27 |
| $(K_2)$ | [mmol kg$_{soil}^{-1}$] | | *2.47* | *2.23* | 2.24 | 2.32 | *2.78* | 2.26 |
| $(Y)$ | [mg mmol$^{-1}$] | | 95.39 | 64.44 | - | - | 305.41 | - |
| $z$ | [mmol mg$^{-1}$] | | 0.01 | 0.01 | - | - | 0.01 | - |
| $\mu$ | [s$^{-1}$] | | $10^{-6}$ | $10^{-6}$ | - | - | $10^{-6}$ | - |
| $S_0$ | [mmol kg$_{soil}^{-1}$] | | 27 | 14.8 | 27 | 14.8 | 55 | 55 |
| $B_0$ | [mg kg$_{soil}^{-1}$] | | 312.42 | 13.45 | - | - | 212.18 | - |
| $E_0$ | [mmol kg$_{soil}^{-1}$] | | - | - | 27.80 | 1.716 | - | 30.71 |